Two-state model for top-of-barrier processes

R. S. Tantawi and A. S. Sabbah
Mathematics Department, Zagazig University, Zagazig, Egypt

J. H. Macek and S. Yu. Ovchinnikov*
Department of Physics and Astronomy, University of Tennessee, Knoxville, Tennessee 37996-1501
and Oak Ridge National Laboratory, Post Office Box 2008, Oak Ridge, Tennessee 37831
(Received 8 March 1999; revised manuscript received 11 February 2000; published 18 September 2000)

A two-state model applicable to top-of-barrier processes in ion-atom collisions at low velocity v is investigated. An expression for the Massey parameter of the transition $n \rightarrow n+1$ is derived and is used to compute ionization, capture, and excitation from states of high principal quantum number in $H^+ + H$ collisions. The Wannier law is obtained at the ionization threshold. The dependence of ionization on the initial n is computed. Total capture cross sections are in good agreement with other calculations, but an unreasonably large fraction goes to resonant capture. It is concluded that multicrossing models, which do not incorporate interference between different paths to the resonant state, overestimate resonant capture.

PACS number(s): 34.80.−i

I. INTRODUCTION

Ionization of atoms in low-velocity, heavy-ion ion collisions has been investigated by several groups [1–5]. Techniques that are sensitive to electrons with energies of the order of 1 eV show that a surprisingly large number emerge in that energy range. These slow electrons have been attributed to a mechanism [6] similar to the one that gives rise to Wannier's threshold law for electron impact ionization of atoms [7–11], even though, for ion impact, the total energy is far above the ionization threshold. In this picture, ionization is possible when the electron is asymptotically at the saddle point of the potential as the nuclei slowly separate. In essence electrons become stranded at the top of a potential barrier between target and projectile and end up ionized with low velocity in the center-of-mass frame. This mechanism will be called the saddle-point or top-of-barrier mechanism. Classical calculations are often employed to describe this process, beginning with the original work of Wannier [7]. Recent *ab initio* quantal calculations based upon direct solution of the time-dependent Schrödinger equation [12,13] are at an early stage and have not provided total cross-section values. The hidden crossing theory [6] gave the first results for top-of-barrier ionization, but none of the quantum calculations have been applied to ionization of states with high principal quantum number n. For ion-atom collisions, classical trajectory Monte Carlo (CTMC) calculations [14] are one of the few methods that give absolute cross sections for high n and at relative velocities that are comparable to the electron velocity in the initial sate.

The first *ab initio* quantum calculations of ionization via the top-of-barrier mechanism in ion-atom collisions employed adiabatic molecular states where a series of broad avoid level crossings were identified. These level crossings are associated with energy levels of Rydberg states that just touch the top-of-barrier at a distance where the potential energy of an electron equals the separated atom energy, up to a factor of the order of unity [11,15]. Absolute cross sections were computed using the hidden-crossing theory [16–18] to treat the multiple crossings, shown schematically in Fig. 1. In this figure a diabatic state with energy equal to $-C_0/R$, where R is the internuclear distance and $C_0 = 4Z-1$ with $Z=1$ for $H^+ + H$, crosses a series of Rydberg states n with energy $\varepsilon_n = Z^2/(2n^2)$. At some distance it is supposed that transitions to the continuum take place. The nature of this transition is obscure. One objective of this investigation is to elucidate the transition to the continuum state.

An important feature of the multicrossing model [19] is that the diabatic curve actually enters the positive energy continuum while the top-of-barrier diabatic curve never actually does so. In effect, transitions to the continuum level are underbarrier transitions. The first section of our manuscript formulates a two-state model to compute direct transitions to positive energy states. We find that the probabilities for such transitions are vanishingly small for high Rydberg states.

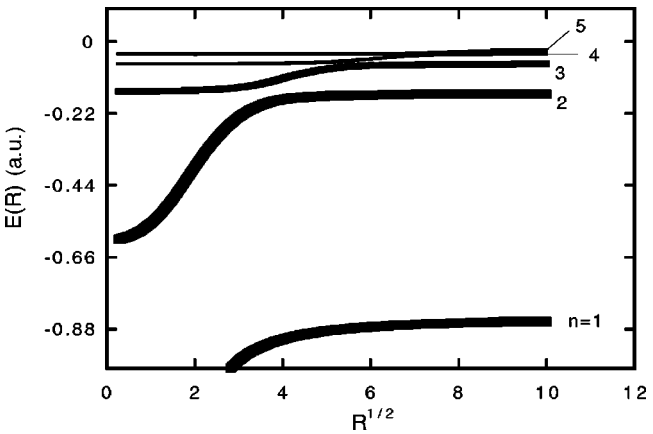

FIG. 1. Schematic plot of adiabatic potential curves showing a series of avoided crossings between Rydberg states and a diabatic energy curve $-C_0/R$.

*Permanent address: Ioffe Physical Technical Institute, St. Petersburg, Russia.

This suggests another interpretation of the diabatic state, namely that it becomes a zero-energy bound state modified by Solov'ev's translation factor $\exp[ir^2/2R(t)]$, asymptotically, where r is the center-of-mass electron coordinate and R is the internuclear distance [20]. Then ionization is computed by evaluating the probability that the diabatic state, denoted here by $|0\rangle$, survives the multiple crossings of the infinitude of Rydberg states. The hidden crossing computations of Ref. [6] employ the probability to survive only a finite number of Rydberg states, i.e., the number of crossings leading to ionization was cut off as some value of n. The closely related theory of Ref. [18] does not employ a cutoff in n, but employs integration of an asymptotic $\varepsilon(R)$ in the complex plane. We show that the survival probability agrees with this later, indirect approach.

The survival probability depends upon the Massey parameter Δ_n for a transition from a Rydberg state to the diabatic state. This quantity is computed in Sec. III where the simple result $\Delta_n = 8/(\pi n^2)$ is found for the states of low magnetic quantum number in $H^+ + H$ collisions. That this expression gives the Wannier threshold law is also demonstrated. An earlier computation using the same method obtained a different law involving powers of $\ln E$. We trace the $\ln E$ terms to an inaccurate expression for the energy difference $\Delta\varepsilon = \varepsilon_{n+1}(R) - \varepsilon_n(R)$ at the crossing radius, thus confirming the surmise of Ref. [18], namely, that the simple estimate $\Delta\varepsilon \propto n^{-3}$ is incorrect.

The Demkov-Osherov [19] multicrossing model employs a projection operator representation of the diabatic potential that varies linearly with time τ. The possibility of solving a similar model that varies as $1/R$, with $R = v\tau$, was also recognized in Ref. [19]. Such a model describes the top-of-barrier diabatic potential curve, however the solution has not been worked out in detail. In this manuscript we report on the solution of a two-state model with a $1/\tau$ diabatic potential $H_{\rm di} = |0\rangle(\beta/\tau)\langle 0|$. Here β is a constant to be determined later, and $|0\rangle$ represents a diabatic state whose explicit form need not be specified.

The model is illustrated schematically in Fig. 2(a). A diabatic potential curve $j = 0$ with a $1/R$ dependence crosses a constant energy curve $j = 1$ representing an excited state. The interaction between the states is modeled by a constant matrix element. Transitions between these states, typically represented by the Landau-Zener model, occur in the vicinity of the crossing of the diabatic curves. We will see that the computed transition matrix elements differ somewhat from those given by the Landau-Zener model. Aside from a factor that is exponentially small for large n, our result agrees with the hidden crossing prescription. If we consider that $j = 1$ is a Rydberg state, then this model, with appropriate values for the model parameters, can be used to compute excitation to high Rydberg states.

As the principal quantum number of the Rydberg states becomes infinite, the $j = 1$ level approaches the zero-energy continuum. Continuum levels are modeled by taking constant positive energy eigenvalues for the excited diabatic state. Transitions to the continuum in this model are represented schematically in Fig. 2(b). Since there is no actual crossing of levels, such transitions are called ''underbarrier'' transitions. In essence the system must tunnel through a forbidden region to pass between asymptotic eigenstates. A two-state model with a $1/\tau$ diabatic potential can model underbarrier transitions. We will obtain closed-form expressions for such transitions in a two-state model.

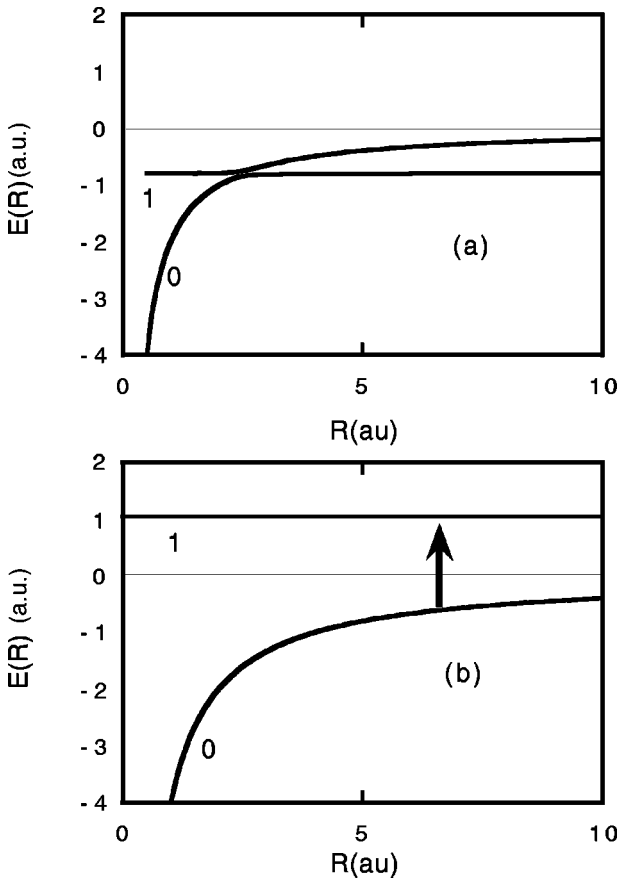

FIG. 2. Schematic plot of adiabatic potential curves for the two-state model with (a) two negative energy states and (b) one negative energy state and a positive energy state.

II. FORMULATION OF THE TWO-STATE MODEL

Our model Schrödinger equation is

$$\left[i\frac{\partial}{\partial\tau} - H_0(\mathbf{q}) - |0\rangle\frac{\beta}{\tau}\langle 0| \right] |\varphi(\mathbf{q},\tau)\rangle = 0, \quad \beta = \beta_0/v, \tag{2.1}$$

where $\mathbf{q}$ is the electron coordinate in the center of charge frame, $H_0(\mathbf{q})$ is the Hamiltonian for an electron in a time-independent potential, β_0 is a constant whose exact value depends upon the physical system to be modeled, and $|0\rangle$ is the diabatic state. Neither the time-independent potential nor the diabatic state $|0\rangle$ need be specified at this point. In order to connect with real diatomic systems, the variable τ will be replaced by $R = v\tau$ in some parts of the discussion.

The solution of the time-dependent equation for general initial conditions is given in terms of the time evolution operator $U(\tau,\tau')$. The matrix elements of this operator taken in the limit as $\tau \to \infty$ and $\tau' \to -\infty$ are just the transition ampli-

tudes in a basis of asymptotic states. The appropriate asymptotic states diagonalize the Hamiltonian

$$H = H_0 + |0\rangle \frac{\beta_0}{R} \langle 0| \tag{2.2}$$

at large values of $|\tau|$.

Equation (2.1) can be solved generally following the methods of Macek and Cavagnero [21]. It turns out that the asymptotic conditions are not easily represented for the general case; thus, we solve the special two-state model defined by

$$\langle 0|H_0|0\rangle = 0, \ \langle 0|H_0|1\rangle = \langle 1|H_0|0\rangle = h, \ \langle 1|H_0|1\rangle = \varepsilon \tag{2.3}$$

by direct solution of the time-dependent equations. The states $j = 0,1$ are the diabatic states of the model. The matrix corresponding to the complete Hamiltonian of Eq. (2.2) in this basis is

$$H = \begin{pmatrix} \frac{\beta_0}{R} & h \\ h & \varepsilon \end{pmatrix}. \tag{2.4}$$

For negative β_0 the eigenvalues of this Hamiltonian are shown schematically in Fig. 1(a) for negative ε and in Fig. 1(b) for positive ε.

The solution of the time-dependent Schrödinger equation, Eq. (2.3) together with Eqs. (2.3) and (2.2), is given quite generally in terms of the time evolution operator $U(\tau,\tau)$,

$$|\varphi(\tau)\rangle = U(\tau,\tau')|\varphi(\tau')\rangle. \tag{2.5}$$

For the two-state model the $U(\tau,\tau')$ is a 2×2 matrix.

The U matrix is obtained in the diabatic basis of states in Appendix A. For $\tau \to 0$ the Hamiltonian is diagonal in diabatic basis, but is not diagonal as $\tau \to \infty$. In order to obtain transition matrix elements it is necessary to use a basis, in which the Hamiltonian is diagonal as $\tau \to \infty$. Since the asymptotic Hamiltonian is diagonal in the adiabatic basis, the transition amplitudes are defined both at $\tau = 0$ and $\tau \to \infty$ in that representation. The transformation to the adiabatic basis is affected by an orthogonal transformation matrix $D(\tau)$ where

$$D(\tau) = \begin{pmatrix} \cos[\theta(\tau)] & \sin[\theta(\tau)] \\ -\sin[\theta(\tau)] & \cos[\theta(\tau)] \end{pmatrix}, \tag{2.6}$$

and where

$$\tan 2[\theta(\tau)] = -\frac{2h}{\beta/\tau - \varepsilon}. \tag{2.7}$$

The matrix that describes the evolution of the system between the times $\tau = \tau_0$, where $\tau_0 \approx 0$ and $\tau \to \infty$, is formally similar to the Jost matrix of time-independent scattering theory [22]. In the time-dependent theory this matrix will be called the ''one-pass'' transition matrix $\mathcal{J}$. It is defined in the basis of adiabatic states as

$$\mathcal{J}_{nm} = \lim_{\tau\to\infty,\tau'\to\tau_0} \exp\left[i \int_{\tau_0}^{\tau} E_n(\tau'')\, d\tau'' \right] \times [D(\tau)^{-1} U(\tau,\tau') D(\tau')]_{nm} \exp\left[i \int_{\tau_0}^{\tau'} E_m(\tau'')\, d\tau'' \right]. \tag{2.8}$$

Defining the quantities

$$\lambda = \sqrt{\varepsilon^2 + 4h^2}, \qquad \nu_0 = \frac{\beta}{2}\left(1 + \frac{\varepsilon}{\lambda}\right), \ \ \nu_1 = \frac{\beta}{2}\left(1 - \frac{\varepsilon}{\lambda}\right), \tag{2.9}$$

and using Eq. (A32) of Appendix A gives $\mathcal{J}$,

$$\mathcal{J}_{00} = -\mathcal{J}_{11}^* = -\sqrt{\frac{\beta}{\nu_1}} \frac{\Gamma(-i\beta)}{\Gamma(-i\nu_1)} \lambda^{i\nu_0} \exp[\pi\nu_0/2],$$
$$\mathcal{J}_{01} = \mathcal{J}_{10}^* = \sqrt{\frac{\beta}{\nu_0}} \frac{\Gamma(-i\beta)}{\Gamma(-i\nu_0)} \lambda^{i\nu_1} \exp[-\pi\nu_1/2]. \tag{2.10}$$

The corresponding transition probabilities are

$$|\mathcal{J}_{00}|^2 = \frac{1 - \exp(-2\pi\nu_1)}{1 - \exp(-2\pi\beta)},$$
$$|\mathcal{J}_{01}|^2 = \frac{\exp(-2\pi\nu_1) - \exp(-2\pi\beta)}{1 - \exp(-2\pi\beta)}. \tag{2.11}$$

Equations (2.10) and (2.11) hold independently of the signs of β and ε. One must recognize, however, that owing to our definition of $D(0)$, it is necessary to interchange $\mathcal{J}_{00}$ and $\mathcal{J}_{01}$ when β is negative. For our applications $\beta = -|\beta|$ and ε can be either negative, as illustrated in Fig. 2(a), or positive, as in Fig. 2(b). In either case we have

$$|\mathcal{J}_{01}|^2 = \frac{\exp(-2\pi|\nu_0|) - \exp(-2\pi|\beta|)}{1 - \exp(-2\pi|\beta|)}. \tag{2.12}$$

If $h \ll \varepsilon$ and $\varepsilon < 0$ we have

$$|\mathcal{J}_{01}|^2 \approx p, \tag{2.13}$$

where

$$p = \exp\left[\frac{-2\pi|\beta_0|}{v} \frac{h^2}{\varepsilon^2} \right]. \tag{2.14}$$

In this case, Eq. (2.14) is the usual two-state Landau-Zener probability. We expect to recover the Landau-Zener result in this limit since the branch point of the adiabatic energy function $E(R)$, i.e., the complex value of R where $E_0(R) = E_1(R)$, is close to the real axis. In this case any two-state model should agree with the Landau-Zener result.

For this model the energy $E(R)$ has branch points at

$$\beta_0/R = -(\varepsilon \pm 2ih). \tag{2.15}$$

According to the hidden crossing theory the probability for a transition is given by $\exp[-2\Delta/v]$, where Δ is the Massey parameter given by

$$\Delta = -\,\mathrm{Im}\int_c E(R)dR, \tag{2.16}$$

where the contour c starts on the real axis on the first sheet of $E(R)$, goes around the branch point, and returns to the real axis on the second sheet. This integral is readily computed for $\varepsilon<0$ and one finds that

$$\Delta = \pi|\nu_0|, \tag{2.17}$$

where ν_0 is given by Eq. (2.9). This result exactly agrees with our solution of the two-state model provided the term $\exp[-2\pi\beta_0/v]$ is neglected. For the applications considered here, this term is always negligible.

For positive ε the transition probability is always less than $\exp[-\pi C_0/v]$. We are interested in processes for which the reduced velocity $v_{\mathrm{rd}}=vn$ is of the order of unity. In that case the direct ionization probability is always less than $\exp[-\pi C_0 n/v_{\mathrm{rd}}]$, which is vanishingly small even for moderate values of n. Thus, direct ionization to the continuum from a state of high n is negligible and the diabatic state $|0\rangle$ itself should be interpreted as a zero energy bound state as $R\to\infty$. With this latter interpretation, ionization is computed by calculating the probability that the state $|0\rangle$ survives multiple crossings of Rydberg states with some nonzero amplitude as $R\to\infty$. Because direct ionization is negligible, and because the present model recovers the hidden crossing transition probability, a multicrossing model treating each transition as independent can be used to compute top-of-barrier processes. Such computations are reported in Sec. III.

III. APPLICATION TO TOP-OF-BARRIER TRANSITIONS

A. Multicrossing theory and model parameters

We wish to apply this model to excitation and ionization of Rydberg states via the top-of-barrier mechanism for $H^+ + H$ collisions. Our first task is to obtain parameters that relate the top-of-barrier branch point to the two-state model. Three parameters—β_0, ε_n, and h_n—for each Rydberg state n are required. An alternative set, namely the Massey parameter Δ_n, the crossing radius R_n, and the asymptotic energy ε_n, relates more closely to the hidden crossing theory, and to cross sections. These latter three parameters are used here as the primary inputs for applications to real physical systems.

For the two-state model we have $|\beta_0|=C_0=4Z-1$, while the top-of-barrier crossing radius has been computed in Ref. [18]. They obtain $R_n=\pi^2n^2/2Z$ for states of even symmetry and zero angular momentum in the separated atom limit. Because $\varepsilon+C_0/R$ must vanish at the crossing, we have

$$\varepsilon_n = -\frac{2C_0Z}{\pi^2n^2} = -\frac{Z_{\mathrm{eff}}^2}{2n^2}, \tag{3.1}$$

which defines Z_{eff}. One sees that $Z_{\mathrm{eff}}\neq Z$, since we have chosen the model energy at the crossing radius rather than at the separated atom limit. The difference is slight with $Z_{\mathrm{eff}}\approx 1.1Z$, and is of no consequence except near the threshold for excitation or capture to a particular final state n_f.

In accord with common practice, the velocity v will be taken to be the radial velocity at the crossing radius. Then one has

$$v(R_n) = \sqrt{v^2+\frac{2C_0}{(MR_n)}-\frac{b^2v^2}{R_n^2}}, \tag{3.2}$$

where M is the reduced mass of the two nuclei, b is the impact parameter, and v now denotes the initial relative velocity.

The remaining parameter of the model is the Massey parameter Δ_n. Approximate expressions for this parameter have been given in the literature, however the available expressions are not sufficiently accurate for our purposes. For that reason, we derive an expression in Appendix B following the analysis of Ref. [18]. There the simple result

$$\Delta_n = \frac{8}{\pi n^2} \tag{3.3}$$

for the H_2^+ system is obtained.

All cross sections for the multicrossing model, illustrated schematically in Fig. 1, can be computed from elements of the time evolution operator $U(-\infty,\infty)$. Constructing this operator directly in the multicrossing model involves tracing all possible transitions or ''paths'' from the initial state n_i to the final state n_f. This is a formidable task [23], even for the simple model given here. Fortunately, this task can be greatly simplified [22] by using the identity

$$U(-\infty,\infty) = U(-\infty,0)U(0,\infty). \tag{3.4}$$

For the operator $U(0,\infty)$, only one path connects a ''united atom'' state n_a near $R=0$ with a separated atom state n_b. It is thus fairly simple to construct the half-collision matrix $U(0,\infty)$. Since time reversal implies the relation

$$|U(-\infty,\infty)|^2 = \left|\sum_{n_a} U_{n_a,n_i}(0,\infty)U_{n_a,n_f}(0,\infty)\right|^2, \tag{3.5}$$

transition probabilities for the physical U matrix are computed simply by matrix multiplication once $U(0,\infty)$ is known.

The sum over intermediate states n_a in Eq. (3.5) is taken coherently. In keeping with the assumptions of the hidden crossing theory, it is supposed that all cross terms average out in the integration over impact parameter so that the coherent sum can be replaced by the incoherent sum

$$|U(-\infty,\infty)|^2 = \sum_{n_a} |U_{n_a,n_i}(0,\infty)|^2|U_{n_a,n_f}(0,\infty)|^2. \tag{3.6}$$

Again, the incoherent sum is readily computed from the half-collision matrix.

The matrix element $|U_{n_a,n_b}(0,\infty)|^2$ is constructed from the two-state transition probabilities p_n where

$$p_n=\exp[-2\Delta_n/v(R_n)] \tag{3.7}$$

if $v(R_n)$ is real, and

$$p_n=0 \tag{3.8}$$

if $v(R_n)$ is imaginary. Let n_x be the smallest value of n for which $v(R_n)$ is real. If n_a is greater than n_x, the system is in a Rydberg state at $\tau=0$, while if $n_a=n_x$ it is in the diabatic state. From Fig. 1 we easily see that if $n_a>n_x$, then

$$\begin{aligned}
&|U_{n_a,n_b}(0,\infty)|^2=(1-p_{n_a-1})p_{n_a}\cdots p_{n_b-1}(1-p_{n_b}),\\
&\qquad n_b>n_a,\\
&|U_{n_a,n_b}(0,\infty)|^2=(1-p_{n_a-1})(1-p_{n_b}),\quad n_b=n_a,\\
&|U_{n_a,n_b}(0,\infty)|^2=p_{n_b},\quad n_b=n_a-1,
\end{aligned} \tag{3.9}$$

while if $na=n_x$ one has

$$\begin{aligned}
&|U_{n_a,n_b}(0,\infty)|^2=p_{n_a}\cdots p_{n_b-1}(1-p_{n_b}),\quad n_b>n_a,\\
&|U_{n_a,n_b}(0,\infty)|^2=(1-p_{n_b}),\quad n_b=n_a.
\end{aligned} \tag{3.10}$$

Since we interpret the diabatic state as an unbound zero-energy state as $R\to\infty$, the probability for a transition from an initial state n_a to the continuum k is given by

$$|U_{n_a,k}(0,\infty)|^2=\lim_{n_b\to\infty}(1-p_{n_a-1})p_{n_a}\cdots p_{n_b}. \tag{3.11}$$

All other elements of $U(0,\infty)$ vanish. This completely defines the matrix $|U_{n_a,n_b}(0,\infty)|^2$. It should be noted that only total ionzation cross sections can be computed in this model.

Collisions of atoms in high Rydberg states with ions are the main focus of this manuscript. As we have seen, these processes depend critically upon the Massey parameter Δ_n. For most ion-atom collisions, the potential term can be neglected in the expression for $v(R_n)$, however as a check on our asymptotic expression for the Massey parameter, we first compute the Wannier threshold law for which the potential term is critical, but the centrifugal term b^2v^2/R_n^2 is neglected.

The probability for the system to stay on the diabatic state after passing the n_fth crossing is

$$P=p_{n_i}p_{n_i+1}\cdots p_{n_f}=\exp[-2S(n_i,n_f)], \tag{3.12}$$

where

$$S(n_i,n_f)=\sum_{n=n_i}^{n_f}\frac{\Delta_n}{v(R_n)} \tag{3.13}$$

and where

$$v(R_n)=\sqrt{2M(E+C_0/R_n)}. \tag{3.14}$$

Substituting our expressions for R_n and Δ_n into the sum, approximating the sum by an integral over n, and writing the results in terms of $\varepsilon_i=C_0/R_{n_i}$ and $\varepsilon_f=C_0/R_{n_f}$ gives

$$S=-8\sqrt{\frac{M}{C_0}}\ln\left[\frac{\sqrt{\varepsilon_f}+\sqrt{\varepsilon_f+E}}{\sqrt{\varepsilon_i}+\sqrt{\varepsilon_i+E}}\right]. \tag{3.15}$$

In the limit as $n_f\to\infty$ or equivalently, $E_f\to 0$, we obtain

$$S=-\zeta_W\ln\sqrt{E}+\zeta_W\ln[\sqrt{\varepsilon_i}+\sqrt{\varepsilon_i+E}]. \tag{3.16}$$

Substituting Eq. (3.16) into Eq. (3.12) gives the well-known Wannier threshold law $\sigma\propto E^{\zeta_W}$ with

$$\zeta_W=\sqrt{\frac{16M}{C_0}}. \tag{3.17}$$

Had we employed hyperspherical coordinates or incorporated a small harmonic-oscillator potential $V_S=C_0r^2/2M$ that originates with Solov'ev's transformation [20], we would obtain

$$\zeta_W\sqrt{\frac{16M}{C_0}+\frac{1}{2}}. \tag{3.18}$$

In order to obtain the correct Wannier exponent, namely

$$\zeta_w=\sqrt{\frac{16M}{C_0}+\frac{9}{16}}-\frac{1}{4}, \tag{3.19}$$

it is necessary to take account of nonadiabatic coupling that is neglected in the present theory. Because the nonadiabatic effects are seen to be of order $1/M$, we conclude that the Massey parameter Δ_n that we compute in Appendix B is accurate for large n. It should be noted that, because atomic units with the mass of the electron $m_e=1$ are used, the mass M in Eq. (3.19) actually stands for the ratio of the reduced mass M of the like charges to the reduced mass of the unlike charge relative to the total mass. These masses are denoted by m_{12} and $m_{12,3}$ in Ref. [9].

It is not our intention to apply this model for $E<0$, since in this region several inconsistencies emerge that can only be corrected by a complete wave treatment. Even so, a brief consideration of this region is useful, if only to demonstrate the limitations of the present theory. For negative E, the diabatic state is populated even after the last energetically allowed channel is passed. One must consider that, in a wave treatment, the outgoing wave in the diabatic channel reaches a turning point, reflects, and return towards the origin [24]. Multiple reflections set up standing waves which have been postulated to give ''ridge'' resonance states [25]. If it is assumed that these states decay mainly to the closest energetically allowed channel n_f, then the probability for the state n_f at an energy just slightly above the asymptotic binding energy $-Z^2/2n_f^2$ is given by Eq. (3.15) with $E=-Z^2/2n_f^2$. Recalling the definition of ε_f, we have

$$|\varepsilon_f| = -\frac{4C_0}{Z\pi^2}E. \tag{3.20}$$

This relationship, and Eq. (3.15), gives a ratio of the ionization probability P_+ at energy E above threshold to the probability P_- for populating n_f at an energy $|E|$ below threshold. The ratio is found to be

$$P_-/P_+ = \left(\sqrt{\frac{4C_0}{Z\pi^2}} + \sqrt{\frac{4C_0}{Z\pi^2}-1}\right)^{2\zeta_W}. \tag{3.21}$$

Equation (3.21) shows that there is a step discontinuity at threshold, with the cross section below threshold being larger than that above, as found earlier [26] and as seen in experiments [28]. The magnitude of the step for $Z=2$ and $M=1/4$, however, is $P_-/P_+=2.65$, which is considerably larger than found experimentally [27]. Decay of ''ridge'' resonances to channels lower than n_f would reduce the ratio, but quantitative computation of this effect is beyond the scope of the present theory.

The remaining applications consider ion-atom interactions at velocities where $E \gg C_0/R$ so that the potential term in $v(R_n)$ is negligible. Extensive computations of ionization, excitation, and charge transfer for these systems are available, however quantitative treatments of the top-of-barrier mechanisms have been restricted to relatively low n. This mechanism is implicitly included in the CTMC theory, but the theory is not applicable when the relative velocity is much lower than the mean electron velocity in the initial state. It is just in this velocity range where the hidden crossing theory should be most reliable.

A truly comprehensive treatment of excitation and ionization for $H^+ + H$ collisions in this framework has been given by Janev and Krstic [23]. To fit our computations into this general framework, we note that the theory of Ref. [23] identifies three types of transitions between adiabatic states, namely united atom rotational coupling, superpromotion, and the top-of-barrier mechanism of interest here. The latter two processes are identified by branch points indicating ''hidden'' crossings of potential curves. One feature that emerges in this theory is that for any adiabatic state, united atom rotational coupling occurs at the smallest values of R, superpromotion next, and finally the top-of-barrier transition at the largest R. This means that the $U(0,\infty)$ matrix can be factored as

$$U(0,\infty) \approx U^{(\mathrm{Rot})}(0,\infty)U^{(S)}(0,\infty)U^{(T)}(0,\infty), \tag{3.22}$$

where the superscripts Rot, S, and T refer to rotational coupling, superpromotion, and top-of-barrier, respectively. This factorization is implicit in Ref. [23] and emerges automatically from asymptotic treatments in $1/v$. This complete matrix is substituted into Eqs. (3.6), where it is important to use

$$U^{(\mathrm{Rot})}(-\infty,\infty) = U^{(\mathrm{Rot})}(-\infty,0)U^{(\mathrm{Rot})}(0,\infty) \tag{3.23}$$

before replacing coherent sums by incoherent sums. With this replacement one then has

$$|U_{n_i,n_f}(-\infty,\infty)|^2 = \sum_{n_a,n_b} |U^{(T)}_{n_a,n_i}(0,\infty)|^2 |U^{(S)}_{n_u,n_a}|^2 \times |U^{(\mathrm{Rot})}_{n_u,n_s}(-\infty,\infty)|^2 |U^{(S)}_{n_s,n_b}(0,\infty)|^2 \times |U^{(T)}_{n_b,n_f}(0,\infty)|^2. \tag{3.24}$$

The squared U matrix for S processes can be written in exactly the same manner as Eqs. (3.9) except that now the transitions always lead to lower states in the half-space $0<t<\infty$. The rotational coupling matrix, however, can only be computed reliably by solving the appropriate coupled-channel equations. We expect that transitions between Rydberg states will be dominated by the top-of-barrier transitions since they occur at the largest crossing radii. For that reason only Eq. (3.5) rather than the more general Eq. (3.24) will be employed in this paper. The error incurred should be less than the ratio of the square of crossing radii of the S and T crossings. The largest crossing radii for the S process is of the order of $2|n^2|$ while it is $\pi^2 n^2/2$ for the T process, thus the error in the cross section is of the order of $8/pi^4 \approx 0.16$. A 16% error is not entirely negligible, but is acceptable.

Conservation rules also emerge in the hidden crossing theory, since at each crossing only certain quantum numbers change. The selection rules for each of the three types of transitions are implicit in the computations of Ref. [23]. For example, united-atom rotational coupling changes the value of $|m|$ while this quantum number is conserved in the S and T transitions. In terms of the parabolic quantum numbers n_ξ, n_η, m one has that $U^{(T)}$ conserves n_ξ and m, $U^{(S)}$ conserves n_η and m, while $U^{(\mathrm{Rot})}$ conserves n_ξ and $n_\eta/2+|m|$. The neglect of rotation and superpromotion therefore implies selection rules that are not exact and may affect the distribution of excited states even though the error in total cross sections is of the order of 16%.

B. Excitation and capture

Excitation cross sections σ_{n_i,n_f} are computed by integrating the squared matrix in element Eq. (3.6) over all impact parameters less than the crossing radius $R_i = R_{n_i}$ for the initial state. The incoherent sum approximation implies that 1/2 of the $n_i \to n_f$ cross section corresponds to excitation or elastic scattering and 1/2 to capture. Thus we have

$$\sigma_{n_i,n_f} = \pi \int_0^{R_i} |U_{n_i,n_f}(-\infty,\infty)|^2 b\,db \tag{3.25}$$

for both excitation and capture.

We have used this equation to compute electron capture and excitation cross sections for a reduced velocity $v_{\mathrm{rd}} = n_i v = 1$ and $n_i = 5,10$. The electron distributions for capture are compared with the loss cross sections from CTMC calculations of Olson [14] in Fig. 3. Loss due to ionization is negligible for purposes of computing total loss, so that equivalent quantities are compared. We see that far more capture occurs to the resonant state $n_f = n_i$ in our model than

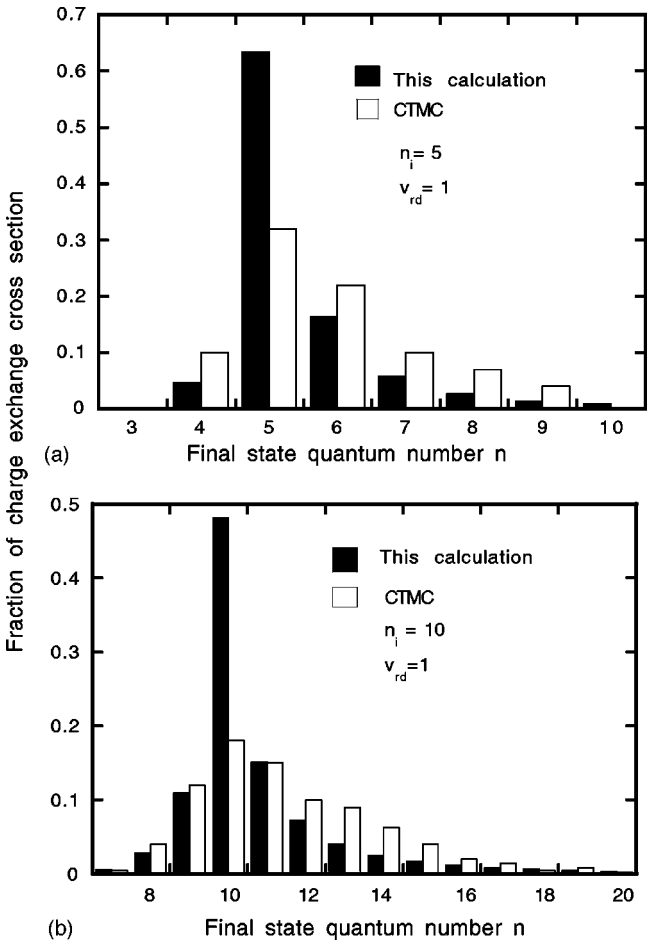

FIG. 3. Comparison of the top-of-barrier and CTMC n distributions for electron capture at a reduced velocity $v_{\mathrm{rd}}=1$ (a) for $n_i=5$ and (b) for $n_i=10$.

in the CTMC calculations. The large resonant capture cross section that we find is easily understood, since the probability for the resonant process is

$$P_{\mathrm{res}}=p_{n_i,n_i}^2+(1-p_{n_i,n_i})^2 \tag{3.26}$$

in the approximation that transitions to lower states are neglected. Because $0<p_{n_i,n_f}<1$, we must have $0.5<P_{\mathrm{res}}<1$, in agreement with the numerical calculations shown in Fig. 3. For $n_i=5$ and $v(r)=v$, it follows that $p_{n_i,n_f}=0.36$ and $P_{\mathrm{res}}=0.54$ in modest agreement with Fig. 3. That we find a slightly smaller probability numerically is mainly due to the variation of $v(r)$ with impact parameter. Similarly $p_{n_i,n_i}=0.6$ for $n_i=10$ so that $P_{\mathrm{res}}=0.52$ in qualitative agreement with the numerical calculations.

The large resonant capture fraction clearly disagrees with the CTMC theory. It also disagrees with the experiments of MacAdam *et al.* [28], suggesting that the hidden crossing theory as presently formulated is inaccurate for high n states. While it is possible that processes neglected in Eq. (3.6) may play some role, they cannot bring our computation of the resonant cross section into accord with the CTMC theory and the data of Ref. [28].

Replacement of the coherent sum by the incoherent sum is probably the main source of error in the present theory. This assumption is usually reliable for processes involving low-lying states, but the present results suggest that it does not apply to states of moderate and high n. Formally, interferences between different terms in Eq. (3.6) are readily taken into account. It is only necessary to keep the phase associated with each channel n_a. It is difficult to do this directly for the $U(-\infty,\infty)$ matrix. The half-collision formulation used here, together with the conservation laws, however, makes such a computation feasible. Even so, it is necessary to have good estimates of all of the potential energy curves in order to compute the phases accurately. Such calculations are beyond the scope of this work.

While the excessively large resonant cross section points to a major flaw in replacing coherent sums by incoherent sums, the other features of the CTMC calculations are reproduced by the top-of-barrier theory. Both distributions show a propensity for populating states with $n_f>n_i$ and both show approximately the same fall-off with increasing n. The slight shoulder seen in the CTMC distributions at $n_f\approx 3n_i/2$ could be due to processes such as rotational coupling, which have been neglected in our calculations, or they could indicate a genuine difference between classical and quantum calculations at $v_{\mathrm{rd}}=1$. In any event, it is necessary to improve the present model in order to investigate this possibility further.

While distributions over final states using the incoherent sum are incorrect, the total capture cross section may not be. The total cross section in the present model is just $\frac{1}{2}\pi R_{n_i}^2$. The estimate $R_n=\pi^2n^2/2$ gives a cross section that appears to be too large. This can be accounted for by employing the more accurate estimate of the crossing radius,

$$R_n=\frac{1}{2}\pi^2 n[n-n_\xi+(|m|+1)/2], \tag{3.27}$$

and averaging R_n^2 over all states. We do this by replacing sums by integrals to find an average squared radius,

$$\langle R_n^2\rangle=\frac{29}{92}R_n^2, \tag{3.28}$$

which gives

$$\sigma^{\mathrm{cap}}=4.9\pi n_i^4 \tag{3.29}$$

in remarkably good agreement with the result $5.5\pi n_i^4$ found in Ref. [14].

C. Ionization

We have already computed ionization cross sections in the threshold region to verify our asymptotic expression for the Massey parameter. It was seen that the multicrossing calculation agreed exactly with the theory of Ref. [18]. That work also computed the ionization probability for velocities where an exponential $P=\exp[-5.11/v]$ was obtained. In the present multicrossing calculation we have for $n=1$ the result $P=\exp[-16/\pi v]=\exp[-5.09/v]$. The close agreement of

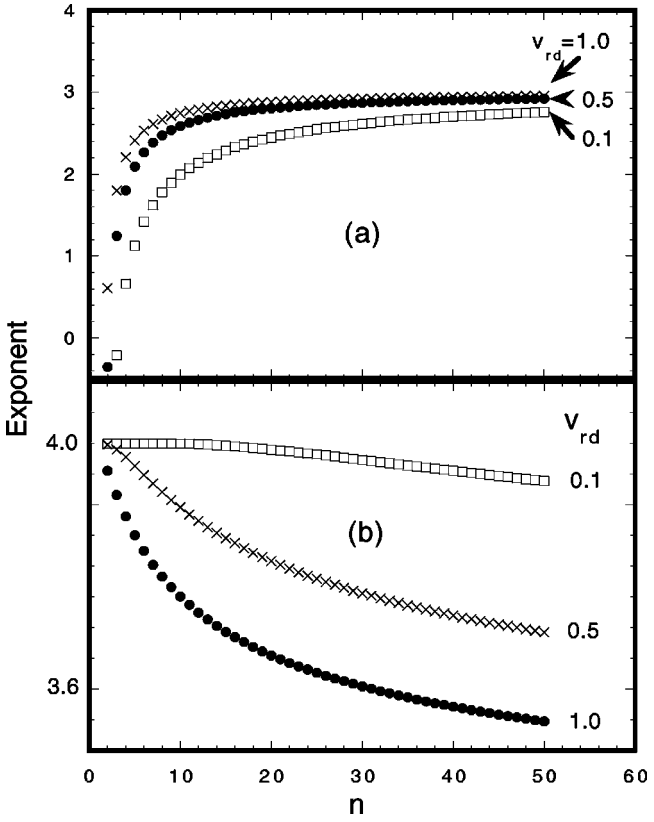

FIG. 4. Plot of the exponent α in the fit $\sigma_{\rm ion}=An^{\alpha}$ of the ionization cross section vs n. The upper plot (a) uses A taken from the value in the limit as $n\to\infty$ with fixed $v_{\rm rd}$ and (b) uses A taken from the limit as $v_{\rm rd}\to 0$ with n fixed.

the Massey parameter in the two theories shows that they are indeed equivalent for total cross sections.

At higher velocities, ionization cross sections as a function of n_i are often fit to a power law $\sigma\propto n^{\alpha}$ for fixed reduced velocity, since this form emerges in most calculations for sufficiently large n and v. The exponent α can be obtained by equating σ to An^{α}, where A is the multiplicative factor in the limit as $n\to\infty$. In this limit

$$\sigma_{n_i}^{(\rm ion)}\to\pi R_{n_i}^2\{1-\exp[-16/(\pi v_{rd}n_i)]\}\exp[-16/(\pi v_{\rm rd})]$$
$$\to\frac{4\pi^4}{v_{\rm rd}}n_i^3\exp[-16/(\pi v_{\rm rd})]. \qquad (3.30)$$

The exponent obtained by fitting the computed $\sigma_n^{(\rm ion)}$ with A from Eq. (3.30) is shown in Fig. 4(a) as a function of the reduced velocity. It is seen that the $\alpha=3$ exponent is approached fairly quickly for reduced velocities of the order of unity, but for $v_{\rm rd}=0.1$ rather high values of n are needed. In addition, the exponent is actually negative, but rapidly varying, for low values of n. In this region, the exponential law with the asymptotic coefficient A is not very informative due to the rapid variation of α with n. Indeed a constant negative value would imply a decreasing cross section, but the rapid increase of α actually gives a cross section that increases with n.

If we consider the limit as $v_{\rm rd}\to 0$, then one finds

$$\sigma_{n_i}^{(\rm ion)}\to\frac{\pi^5}{4}n_i^4\exp[-16/\pi v_{\rm rd}]. \qquad (3.31)$$

With $A=(\pi^5/4)n_i^4\exp[-16/\pi v_{\rm rd}]$, a plot [see Fig. 4(b)] of the fitted α starts out at $\alpha=4$ for low values of n and decreases slowly with increasing n. The decrease towards $\alpha=3$ is more rapid for larger $v_{\rm rd}$ but never actually equals 3 in the range of n values shown. This shows that the exponent and the coefficient in the power law An^{α} are not independent. For moderate values of both $v_{\rm rd}$ and n, the power law is useful but it must be understood that empirically computed power laws may not be valid for infinite n, since the constant in that limit is generally not known.

IV. CONCLUSIONS

We have solved a two-state model for ionization and excitation to Rydberg states, applicable when one of the diabatic potential curves approaches the continuum manifold at infinite distances as $\varepsilon(R)=-C_0/R$. When two potential curves actually cross, the transition probabilities agree with the Landau-Zener and the hidden crossing models in the weak-coupling limit. Direct transitions to positive energy states are also computed in this model and are found to be vanishingly small for fixed reduced velocity and large n_i. Ionization is therefore computed in terms of the probability that the diabatic state survives to infinite R. To apply the theory, an asymptotic expression for the Massey parameter was computed. We find a remarkably simple expression $\Delta_n=8/\pi n^2$, which corrects an earlier result. This expression gives the accepted form for the Wannier threshold law.

Ionization cross sections were computed for a variety of initial principal quantum numbers n_i and were fit to a power law An_i^{α} at fixed reduced velocity. Asymptotic values of A and α for large n_i were extracted and compared with our numerical calculations. It is found that the asymptotic exponent $\alpha=3$ is approached very slowly. Over most of the velocity range where the model is applicable, an exponent $\alpha=4$ gives a better fit. This power law emerges in the limit $v_{\rm rd}\to 0$ with n_i large but fixed.

Electron capture cross sections for $H^+ + H$ collisions were computed for $n_i=5$ and $n_i=10$. The distribution over n values showed an unrealistically large fraction for resonant charge transfer. This large fraction suggests that the use of an incoherent sum over paths, well accepted for processes involving low n states, is incorrect for high n. Total cross sections which are sensitive only to the crossing radius in this model agree within 10% with CTMC results. We conclude that the dynamics of high Rydberg states are indeed governed mainly by the top-of-barrier mechanism, but that the present formulation of the hidden crossing theory must be extended to include phase information normally omitted in that theory.

ACKNOWLEDGMENTS

S.O. and J.M. acknowledge support by the Division of Chemical Sciences, Office of Basic Energy Sciences, Office of Energy Research, U.S. Department of Energy through a

grant to Oak Ridge National Laboratory, which is managed by Lockheed Martin Energy Research Corp. under Contract No. DE-AAC05-96OR22464 with the U.S. Department of Energy. J.M. also gratefully acknowledges support by the National Science Foundation under Grant No. PHY-9600017. R.M.T. is financially supported by the Egyptian Ministry of Education.

APPENDIX A: THE *U* MATRIX

To evaluate $U(\tau,\tau')$ we project Eq. (2.1) onto $|0\rangle,|1\rangle$ and use Eq. (2.3) to obtain the system of differential equations,

$$\left(i\frac{\partial}{\partial\tau}-\frac{\beta}{\tau}\right)a_0(\tau)-ha_1(\tau)=0, \tag{A1}$$

$$\left(i\frac{\partial}{\partial\tau}-\varepsilon\right)a_1(\tau)-ha_0(\tau)=0. \tag{A2}$$

The adiabatic energy levels are given by

$$E_{0,1}(\tau)=\frac{1}{2}[\varepsilon+\beta/\tau\pm\sqrt{(\beta/\tau-\varepsilon)^2+4h^2}]. \tag{A3}$$

As $\tau\to\infty$ we get

$$E_0\sim\omega_0-\frac{\omega_1}{\lambda}\frac{\beta}{\tau},\quad E_1\sim\omega_1+\frac{\omega_0}{\lambda}\frac{\beta}{\tau}, \tag{A4}$$

where $\omega_0=(\varepsilon+\lambda)/2$, $\omega_1=(\varepsilon-\lambda)/2$, and $\lambda=\sqrt{\varepsilon^2+4h^2}$.

To solve Eq. (A1) and Eq. (A2), let

$$a_{0,1}(\tau)=d_{0,1}(\tau)\exp\left[-i\frac{\beta}{2}\int^{\tau}\frac{d\tau'}{\tau'}\right], \tag{A5}$$

then $d_{0,1}(\tau)$ satisfy

$$\left(i\frac{\partial}{\partial\tau}-\frac{\beta}{2\tau}\right)d_0(\tau)=hd_1(\tau) \tag{A6}$$

and

$$\left(i\frac{\partial}{\partial\tau}+\frac{\beta}{2\tau}\right)d_1(\tau)=hd_0(\tau)+\varepsilon d_1(\tau). \tag{A7}$$

Operating on Eq. (A7) by $[i(\partial/\partial\tau)-(\beta/2\tau)]$ and replacing $d_0(\tau)$ from Eq. (A6), and then taking $d_1(\tau)=e^{-i(\varepsilon/2)\tau}y(\tau)$ in the new equation gives

$$\frac{\partial^2y(\tau)}{\partial\tau^2}+\left(h^2+\frac{\varepsilon^2}{4}-\frac{\varepsilon\beta}{2\tau}+\frac{\frac{\beta^2}{4}+\frac{i\beta}{2}}{\tau^2}\right)y(\tau)=0. \tag{A8}$$

Letting $\tau=\alpha x$, the above equation gives

$$\frac{\partial^2y(x)}{\partial x^2}+\left(\alpha^2\left[h^2+\frac{\varepsilon^2}{4}\right]-\frac{\alpha\varepsilon\beta}{2x}+\frac{\frac{\beta^2}{4}+\frac{i\beta}{2}}{x^2}\right)y(x)=0. \tag{A9}$$

Upon setting $\alpha^2[h^2+(\varepsilon^2/4)]=-\frac{1}{4}$ [i.e., $\alpha=-(i/\lambda)$], $k=i\varepsilon\beta/(2\lambda)$, and $\mu=i\beta/2-1/2$, the above equation takes the form

$$\frac{\partial^2y(x)}{\partial x^2}+\left(-\frac{1}{4}+\frac{k}{x}+\frac{\frac{1}{4}-\mu^2}{x^2}\right)y(x)=0, \tag{A10}$$

which is Whittaker's equation [29] with solutions $M_{k,\pm\mu}(x)$. It follows that Eqs. (A1) and (A2) have the solution array

$$f_{00}(\tau)=\frac{1}{h}\left(i\frac{\partial}{\partial\tau}-\varepsilon\right)f_{10}(\tau), \tag{A11}$$

$$f_{01}(\tau)=\frac{1}{h}\left(i\frac{\partial}{\partial\tau}-\varepsilon\right)f_{11}(\tau), \tag{A12}$$

$$f_{10}(\tau)=e^{(-i\varepsilon/2)\tau}e^{(-i\beta/2)\int^{\tau}(d\tau'/\tau')}M_{(i\varepsilon\beta/2\lambda),(i\beta/2)-(1/2)}(i\lambda\tau), \tag{A13}$$

$$f_{11}(\tau)=e^{(-i\varepsilon/2)\tau}e^{(-i\beta/2)\int^{\tau}(d\tau'/\tau')}M_{(i\varepsilon\beta/2\lambda),(-i\beta/2)+(1/2)}(i\lambda\tau). \tag{A14}$$

Now using the definition to the time evolution matrix $U(\tau,\tau')$, namely

$$f(\tau)=U(\tau,\tau')f(\tau'), \tag{A15}$$

we find, using $U(\tau,\tau')=f(\tau)f(\tau')^{-1}$, the result

$$U_{ii}=[f_{ii}(\tau)f_{jj}(\tau')-f_{ij}(\tau)f_{ji}(\tau')]/d(\tau'),\quad i=0,1;\quad j=1,0,$$

$$U_{ij}=[-f_{ii}(\tau)f_{ij}(\tau')+f_{ij}(\tau)f_{ii}(\tau')]/d(\tau'), \tag{A16}$$

where

$$d(\tau')=f_{00}(\tau')f_{11}(\tau')-f_{01}(\tau')f_{01}(\tau')$$

$$=\frac{(i+\beta)\lambda}{h}\exp(-i\beta\ln\tau'+i\omega_0\tau'). \tag{A17}$$

To evaluate Whittaker's functions we use

$$M_{k,\mu}(z)=z^{\mu+1/2}e^{-z/2}{}_1F_1(\mu-k+1/2,2\mu+1,z) \tag{A18}$$

and

$$\frac{d}{dz}{}_1F_1(a,b,z)=\frac{a}{b}{}_1F_1(a+1,b+1,z), \tag{A19}$$

where ${}_1F_1(a,b,z)$ is the confluent hypergeometric function, to obtain the expressions

$$f_{00}(\tau)=\omega_1 h^{-1}(i\lambda)^{i\beta/2}e^{-i\omega_0\tau}[\,{}_1F_1(1-i\beta\omega_1/\lambda,1+i\beta,i\lambda\tau) - {}_1F_1(-i\beta\omega_1/\lambda,i\beta,i\lambda\tau)], \tag{A20}$$

$$f_{01}(\tau)=(i\lambda)^{1-i\beta/2}h^{-1}\exp\left[-i\omega_0\tau-i\beta\int^{\tau}\frac{\tau'}{\tau'}\right] \times\left[(i+\beta-\omega_1\tau)\,{}_1F_1(1-i\beta\omega_0/\lambda,2-i\beta,i\lambda\tau) - \tau\frac{\lambda-i\beta\omega_0}{2-i\beta}\,{}_1F_1(2-i\beta\omega_0/\lambda,3-i\beta,i\lambda\tau)\right], \tag{A21}$$

$$f_{10}(\tau)=(i\lambda)^{i\beta/2}e^{-i\omega_0\tau}\,{}_1F_1(-i\beta\omega_1/\lambda,i\beta,i\lambda\tau), \tag{A22}$$

and

$$f_{11}(\tau)=(i\lambda)^{1-i\beta/2}\tau\exp\left[-i\omega_0\tau-i\beta\int^{\tau}\frac{d\tau'}{\tau'}\right] \times {}_1F_1(1-i\beta\omega_0/\lambda,2-i\beta,i\lambda\tau). \tag{A23}$$

Since ${}_1F_1(a,b,0)=1$, then as $\tau'\to 0$ we have

$$f_{00}(\tau')=f_{11}(\tau')=0,$$

$$f_{01}(\tau')=\frac{i+\beta}{h}(i\lambda)^{1-i\beta/2}(\tau')^{-i\beta}\exp[-i\omega_0\tau'], \tag{A24}$$

$$f_{10}(\tau')=(i\lambda)^{i\beta/2}\exp[-i\omega_0\tau'],$$

therefore, as $\tau'\to 0$ we obtain

$$U_{00}(\tau,\tau')=\frac{f_{01}(\tau)}{f_{01}(\tau')},\quad U_{01}(\tau,\tau')=\frac{f_{00}(\tau)}{f_{10}(\tau')}, \tag{A25}$$

$$U_{10}(\tau,\tau')=\frac{f_{11}(\tau)}{f_{01}(\tau')},\quad U_{11}(\tau,\tau')=\frac{f_{10}(\tau)}{f_{10}(\tau')}.$$

Since, as $z\to\infty$,

$${}_1F_1(a,b,z)\to\Gamma(b)\left(\frac{e^{\pm i[|z|-(\pi/2)(b-a)]}}{\Gamma(a)}|z|^{a-b} + \frac{e^{\pm(i\pi/2)a}}{\Gamma(b-a)}|z|^{-a}\right), \tag{A26}$$

where $z=\pm i|z|$, then, as $\tau\to\infty$, we obtain

$$f_{00}(\tau)=-\frac{\Gamma(i\beta)}{h}(i\lambda)^{i\beta/2}\left[\omega_0\frac{e^{-i\omega_1\tau+(\pi\beta\omega_0/2\lambda)}}{\Gamma\left(-i\frac{\beta\omega_1}{\lambda}\right)}(\lambda\tau)^{-i\beta\omega_0/\lambda} + \omega_1\frac{e^{-i\omega_0\tau+(\pi\beta\omega_1/2\lambda)}}{\Gamma\left(i\frac{\beta\omega_0}{\lambda}\right)}(\lambda\tau)^{i\beta\omega_1/\lambda}\right], \tag{A27}$$

$$f_{01}(\tau)=i\frac{\Gamma(2-i\beta)}{\lambda h}(i\lambda)^{1-i(\beta/2)} \times\left[-\omega_1\frac{e^{-i\omega_0\tau+(\pi\beta\omega_0/2\lambda)}}{\Gamma\left(1+i\frac{\beta\omega_1}{\lambda}\right)}\lambda^{i\beta\omega_0/\lambda}\tau^{i\beta\omega_1/\lambda} + \omega_0\frac{e^{-i\omega_1\tau+(\pi\beta\omega_1/2\lambda)}}{\Gamma\left(1-i\frac{\beta\omega_0}{\lambda}\right)}\lambda^{-i\beta\omega_1/\lambda}\tau^{-i\beta\omega_0/\lambda}\right], \tag{A28}$$

$$f_{10}(\tau)=\Gamma(i\beta)(i\lambda)^{i\beta/2}\left[\frac{e^{-i\omega_1\tau+(\pi\beta\omega_0/2\lambda)}}{\Gamma\left(-i\frac{\beta\omega_1}{\lambda}\right)}(\lambda\tau)^{-i\beta\omega_0/\lambda} + \frac{e^{-i\omega_0\tau+(\pi\beta\omega_1/2\lambda)}}{\Gamma\left(i\frac{\beta\omega_0}{\lambda}\right)}(\lambda\tau)^{i\beta\omega2/\lambda}\right], \tag{A29}$$

$$f_{11}(\tau)=-i\frac{\Gamma(2-i\beta)}{\lambda}(i\lambda)^{1-i(\beta/2)} \times\left[\frac{e^{-i\omega_1\tau+(\pi\beta\omega_1/2\lambda)}}{\Gamma\left(1-i\frac{\beta\omega_0}{\lambda}\right)}\lambda^{-i\beta\omega_1/\lambda}\tau^{-i\beta\omega_0/\lambda} - \frac{e^{-i\omega_0\tau+(\pi\beta\omega_0/2\lambda)}}{\Gamma\left(1+i\frac{\beta\omega_1}{\lambda}\right)}\lambda^{i\beta\omega_0/\lambda}\tau^{i\beta\omega_1/\lambda}\right]. \tag{A30}$$

We therefore obtain

$$U_{ij}(\infty,0)=\lim_{\tau\to\infty}\lim_{\tau'\to 0}\left(A_{ij}\exp\left[-i\int^{\tau}d\tau' E_0(\tau')\right] + B_{ij}\exp\left[-i\int^{\tau}d\tau' E_2(\tau')\right]\right) \times\exp(i\omega_0\tau'+i\delta_{j0}\beta\ln\tau'), \tag{A31}$$

which shows that the matrix elements $U_{nm}(\infty,0)$ are linear combinations of adiabatic amplitudes, where

$$A_{00}=\cot(\theta)A_{10}=\frac{\Gamma(-i\beta)}{\Gamma(-i\nu_1)}\lambda^{i\nu_0}\exp(\pi\nu_0/2),$$

$$A_{11}=\tan(\theta)A_{01}=\frac{\Gamma(i\beta)}{\Gamma(i\nu_0)}\lambda^{-i\nu_1}\exp(-\pi\nu_1/2),$$

$$B_{00}=-\tan(\theta)B_{10}=A_{11}^*, \tag{A32}$$

$$B_{11}=-\cot(\theta)B_{01}=A_{00}^*,$$

and where $\nu_j=\omega_j/(\beta\lambda)$ and θ is given by Eq. (2.9) of Sec. II.

APPENDIX B: THE MASSEY PARAMETER FOR TOP-OF-BARRIER TRANSITIONS

The Massey parameter for transitions at crossings of potential curves is defined in terms of the probability for transition p according to

$$p=\exp[-2\Delta/v]. \tag{B1}$$

The exponential transition probability follows from Landau-Zener and other multicrossing models, however the hidden crossing theory is the most general context for this representation. In that theory transitions are computed by integrating the phase integral

$$\frac{\Delta}{v}=\mathrm{Im}\int\frac{\varepsilon(R)}{v(R)}dR \tag{B2}$$

along a path in the complex plane such that the adiabatic energy function $E(R)$ starts with the value ε_i on the real axis at small R and ends up with the value ε_f on the real axis in the $R\to\infty$ limit. This can only happen if the path goes around a branch point connecting two sheets, i and f, of the Riemann surface of $\varepsilon(R)$. The position of the branch point R_c and the phase integral are critical quantities that we will compute in this appendix for the top-of-barrier hidden crossings.

The energy eigenvalues $\varepsilon(R)$ near the top of a potential barrier have been treated semiclassically by Macek and Ovchinnikov [18]. Their Eq. (B14) for symmetric systems such as H_2^+ is used as the starting point for the computation of Δ_n. They give

$$\phi(R)+\arg\Gamma\{[2\pm1+i2a(R)]/4\}-iQ(R)a(R)=\pi(n+1/2\mp1/8), \tag{B3}$$

where $\phi(R)$ is a WKB phase integral,

$$\phi(R)=\int_0^{1/2}\sqrt{2R^2[C_0/R-V(R,x)]}dx,$$

$$V(R,x)=\frac{1}{R}\left(-\frac{Z}{|1/2-x|}-\frac{Z}{|1/2+x|}+1\right), \tag{B4}$$

and $a(R)$ and $Q(R)$ are given by

$$a(R)=\sqrt{R^3/32Z}(-C_0/R-\varepsilon),$$

$$Q(R)=\frac{1}{4}\ln[32ZR]-1. \tag{B5}$$

For the specific potential of interest here,

$$\phi(R)=32Z/R,\quad a(R)=\frac{R^{3/2}}{\sqrt{32Z}}(C_0/R-\varepsilon). \tag{B6}$$

The position of the branch point R_n corresponding to a given n was found in Ref. [18] from the quantization condition Eq. (B3). They obtain

$$\mathrm{Re}\,R_n=\pi^2n^2/2Z,$$

$$\mathrm{Im}\,R_n=\frac{3\pm1}{2}\sqrt{\frac{2\,\mathrm{Re}\,R_n}{Z}}\left[\frac{1}{4}\ln\left(\frac{2^9Z\,\mathrm{Re}\,R_n}{\pi^2}\right)+\ln\left(\frac{1}{2}\ln(2^7\mathrm{Re}\,R_n)-2+\gamma\right)\right], \tag{B7}$$

where γ is Euler's constant and $\pm$ refers to gerade and ungerade states, respectively.

The Massey parameter is found by integrating $\varepsilon(R)$, given implicitly by Eq. (B3), around a path on the real axis that starts at $R=\mathrm{Re}\,R_n$, goes around the branch point, and ends at $R=\mathrm{Re}\,R_{n+1}$. This integral is approximated by the product of 2 $\mathrm{Im}\,R_n$ and $\Delta\varepsilon=\varepsilon_{n+1}(R)-\varepsilon_n(R)$. A simple estimate of the energy difference, namely $\Delta\varepsilon=-C_0(1/R_n-1/R_{n+1})$, was used in Ref. [10], but this estimate is not sufficiently accurate for large values of n. A more accurate value is derived here.

Since $a\approx0$ at the top-of-barrier, an estimate of $\Delta\varepsilon$ for large n is found by expanding the quantization condition about the point $a=0$ to obtain

$$\phi(R)+[\psi((2\pm1)/4)/2+Q(R)]a=\pi(n+1/2\pm1/8). \tag{B8}$$

The difference $\Delta\varepsilon$ is readily found to be

$$\Delta\varepsilon=\sqrt{\frac{32Z}{R^3}}\frac{\pi}{Q(R)+\psi((2\mp1)/4)/2}. \tag{B9}$$

The Massey parameter is then

$$\Delta(R_n)=\frac{4\pi}{R_n}\left[(2\mp1)+O\left(\frac{1}{\ln R_n}\right)\right]. \tag{B10}$$

Substituting $R_n=\pi^2n^2/2Z$ into Eq. (B10) and specializing to even symmetry gives the expression

$$\Delta_n=\frac{8Z}{\pi n^2} \tag{B11}$$

used in Sec. III.

[1] M.B. Shah, D.S. Elliot, and H.B. Gilbody, J. Phys. B **20**, 2481 (1987).
[2] R. Dörner, H. Khemliche, M.H. Prior, C.L. Cocke, J.A. Gary, R.E. Olson, V. Mergel, J. Ullrich, and H. Schmidt-Böcking, Phys. Rev. Lett. **77**, 4520 (1996).
[3] M. Pieksma, S.Yu. Ovchinnikov, J. van Eck, W.B. Westerveld, and A. Niehaus, Phys. Rev. Lett. **73**, 46 (1994).
[4] M.A. Abdalla, W. Wolff, C.L. Cocke, and M. Stöckli, Phys. Rev. A **58**, R3379 (1998).
[5] G.N. Ogurtsov, A.G. Kroupyshev, M.G. Sargsyan, Y.S. Gordeev, and S.Yu. Ovchinnikov, Phys. Rev. A **53**, 2391 (1996).
[6] M. Pieksma and S.Y. Ovchinnikov, J. Phys. B **24**, 3865 (1991).
[7] G.H. Wannier, Phys. Rev. **90**, 3071 (1953).
[8] A.R.P. Rau, Phys. Rev. A **4**, 207 (1971).
[9] J.M. Feagin, J. Phys. B **17**, 2433 (1984).
[10] S.Yu. Ovchinnikov, Phys. Rev. A **42**, 3865 (1990).
[11] U. Fano, Rep. Prog. Phys. **46**, 97 (1983).
[12] J.C. Wells, D.R. Schultz, P. Gavras, and M.S. Pindzola, Phys. Rev. A **54**, 593 (1996).
[13] E.Y. Sidsky and C.D. Lin, Phys. Rev. A **60**, 377 (1999).
[14] R.E. Olson, J. Phys. B **13**, 483 (1980).
[15] J.M. Rost, J.S. Briggs, and P.T. Greenland, J. Phys. B **22**, L353 (1989).
[16] E.A. Solov'ev, Usp. Fiz. Nauk. **157**, 437 (1989) [Sov. Phys. Usp. **32**, 228 (1989)].
[17] S.Yu. Ovchinnikov and E.A. Solov'ev, Comments At. Mol. Phys. **XXII**, 69 (1988).
[18] J.H. Macek and S.Yu. Ovchinnikov, Phys. Rev. A **49**, R4273 (1994).
[19] Yu.N. Demkov and V.I. Osherov, Zh. Éksp. Teor. Fiz. **53**, 1589 (1967) [Sov. Phys. JETP **26**, 916 (1968)].
[20] E.A. Solov'ev and S.I. Vinitsky, J. Phys. B **18**, L557 (1985).
[21] J.H. Macek and M.J. Cavagnero, Phys. Rev. A **58**, 348 (1998).
[22] J.H. Macek, in *Fundamental Processes of Atomic Dynamics*, *NATO Advanced Study Institute Series*, edited by J.S. Briggs, H. Kleinpoppen, and H.O. Lutz (Plenum, New York, 1988), pp. 129–142.
[23] R.K. Janev and P.S. Krstic, Phys. Rev. A **46**, 5554 (1992).
[24] U. Fano, J. Phys. B **13**, L519 (1980).
[25] A.R.P. Rau, J. Phys. B **16**, L699 (1983).
[26] H.R. Sadeghpour, Bull. Am. Phys. Soc. **39**, 1225 (1994) and private communication.
[27] S. Cvejanovic, R. Shiell, and T.S. Reddish, J. Phys. B **28**, L707 (1996).
[28] K.B. MacAdam, L.G. Gray, and R.G. Rolfes, Phys. Rev. A **42**, 5269 (1990).
[29] *Handbook of Mathematical Functions*, edited by Milton Abramowitz and Irene A. Stegun (National Bureau of Standards, Washington, D.C., 1964).